Interdependence of particle properties and bulk powder behavior of indomethacin in quench-cooled molten two-phase solid dispersions

Kristian Semjonov, Maia Salm, Tiina Lipiäinen, Karin Kogermann, Andres Lust, Ivo Laidmäe, Osmo Antikainen, Clare J. Strachan, Henrik Ehlers, Jouko Yliruusi, Jyrki Heinämäki

PII: S0378-5173(18)30120-0
DOI: https://doi.org/10.1016/j.ijpharm.2018.02.039
Reference: IJP 17337

To appear in: *International Journal of Pharmaceutics*

Received Date: 18 December 2017
Revised Date: 20 February 2018
Accepted Date: 21 February 2018

Please cite this article as: K. Semjonov, M. Salm, T. Lipiäinen, K. Kogermann, A. Lust, I. Laidmäe, O. Antikainen, C.J. Strachan, H. Ehlers, J. Yliruusi, J. Heinämäki, Interdependence of particle properties and bulk powder behavior of indomethacin in quench-cooled molten two-phase solid dispersions, *International Journal of Pharmaceutics* (2018), doi: https://doi.org/10.1016/j.ijpharm.2018.02.039

Interdependence of particle properties and bulk powder behavior of indomethacin in quench-cooled molten two-phase solid dispersions

Kristian Semjonov[1*], Maia Salm[1], Tiina Lipiäinen[2], Karin Kogermann[1], Andres Lust[1], Ivo Laidmäe[1], Osmo Antikainen[2], Clare J. Strachan[2], Henrik Ehlers[2], Jouko Yliruusi[2], and Jyrki Heinämäki[1]

[1]Institute of Pharmacy, Faculty of Medicine, University of Tartu, Nooruse Str. 1, EE-50411 Tartu, Estonia

[2]Division of Pharmaceutical Chemistry and Technology, Faculty of Pharmacy, University of Helsinki, Viikinkaari 5E, FI-00014 University of Helsinki, Finland

Corresponding Author:

Kristian Semjonov

Institute of Pharmacy, Faculty of Medicine, University of Tartu,

Nooruse Str. 1, EE-50411 Tartu, Estonia

Telephone: +372 51980454

Fax: +372 7375289

Email: kristian.semjonov@ut.ee

Abstract

Solid dispersions (SDs) hold a proven potential in formulating poorly water-soluble drugs. The present paper investigates the interfacial phenomena associated with the bulk powder flow, water sorption, wetting and dissolution of the SDs prepared by a modified melt and quench-cooling (QC) method. Poorly water-soluble indomethacin (IND) was QC molten with solubilizing graft copolymer (Soluplus®) or polyol sugar alcohol (xylitol, XYL). The interfacial interactions of SDs with air/water were found to be reliant on the type (amorphous/crystalline) and amount of the carrier material used. The final SDs were composed of fused agglomerates (SOL) or large jagged particles (XYL) with good wetting and powder flow properties. The initial dissolution of IND was accelerated by both carrier materials studied. The QC molten SDs with amorphous Soluplus® significantly improved the dissolution rate of IND at pH 6.8 (79.9 ± 0.2% at 30 min) compared to that of pure crystalline drug. The substantial improvement in the dissolution rate of IND was in connection with the amorphous state of the drug being stabilized by Soluplus® in the QC molten SDs. However, it is evident that a strong H-bond formation between the components in some regions of the QC molten SDs can limit the dissolution of IND. The QC molten two-phase SDs with a polyol carrier (XYL) showed rapid and continuous drug release without reaching a plateau.

Keywords: particle **properties**, **bulk powder behavior**, dissolution, solid dispersion, polymer

1. INTRODUCTION

Since the early 1960´s, pharmaceutical solid dispersions (SDs) have been brought up as a potential alternative formulation approach for poorly water-soluble drugs. In the well-known pioneering study, Sekiguchi and Obi (1961) discovered that the oral administration of eutectic mixtures of sulfathiazole and urea (obtained by a co-fusion method) resulted in enhanced drug absorption in healthy adults compared to sulfathiazole alone (Sekiguchi and Obi, 1961). Within the next two-three decades, interest in pharmaceutical SDs was steadily increased due to the encouraging reports on the use of SDs with poorly soluble drugs. More recently, the next generation SDs containing surfactant carrier(s) and/or amorphous polymer(s) have been introduced (Vasconcelos et al., 2007).

In pharmaceutical sciences, the term "SD" refers to both solid one-phase homogeneous molecular mixtures and phase-separated suspended mixtures of drug and inert carrier material (Leuner and Dressman, 2000; Thommes et al., 2011; Williams et al., 2013). The present systems have different miscibility of the components, different dissolution behavior and physical stability, and they are prepared with different methods (Leuner and Dressman, 2000; Williams et al. 2013). In one-phase SDs, the drug and carrier material are molecularly dispersed, thus forming a homogeneous glass solution (amorphous carrier) or solid solution (crystalline carrier) type SDs (Leuner et al, 2000; Williams et al., 2013). Two-phase or otherwise multi-phase SDs consist of non-miscible or partially miscible crystalline/amorphous or amorphous/amorphous phases (Thommes et al., 2011). **Depending on the conditions during preparation components may remain poorly miscible or phase separate into polymer and drug rich areas.**

The desired SD structure for improving drug dissolution would be one-phase homogeneous solid solution (Brough and Williams, 2013). However, the opposite effect has been

observed with one-phase SDs with no detectable drug dissolution due to the formation hydrogen bonds between the drug and carrier material (Surwase et al., 2015). Two-phase glassy suspensions and amorphous precipitation systems may circumvent this problem, and thus, they have also a great potential to achieve these goals (Thommes et al., 2011; Thommes, 2012). In addition, two-phase systems enable to incorporate higher drug loadings in a SD matrix. Several *in-vivo* studies confirm the improved dissolution rate and bioavailability of amorphous SDs (Xie at al., 2008; DiNunzio et al., 2010; Williams et al., 2013). **The dissolution and physical stability of the two-component SDs are dependent on the drug-polymer interactions (Semjonov et al., 2017; Thommes, 2012; Thommes et al., 2011; Van Den Mooter, 2012).** According to the literature, approximately 82% of amorphous SDs (both one and/two phases systems) promoted the bioavailability of a poorly water-soluble drug (Newman et al., 2012).

Pharmaceutical SDs are commonly fabricated with melt or solvent evaporation methods (Leuner and Dressman, 2000; Vasconcelos et al., 2007). With a melt (co-fusion) method, melting temperature, mixing efficiency, cooling rate, and the type and viscosity of a carrier polymer are critical variables affecting the homogeneity and physical stability of SDs (Leuner and Dressman, 2000; Vasconcelos et al., 2007; Janssens and Van den Mooter, 2009). For example, too high melting temperatures can accelerate thermal decomposition or evaporation of the drug. The ideal carrier for the melt method has the following characteristics: inert, thermostable, high glass transition temperature (T_g), soluble in water, and capable for solubilizing and stabilizing drugs. In our previous study, we showed that melting the drug first, and then adding a carrier material with subsequent quench cooling (QC) resulted in two-phase amorphous systems with a moderate physical stability (Semjonov et al., 2017). Soluplus® graft copolymer (polyvinyl caprolactam-polyvinyl acetatepolyethylene glycol) (BASF, Soluplus® – Technical Information, 2012) and freely water-soluble xylitol (XYL) were used as carrier materials. Soluplus® (SOL) is a

thermostable and thermoplastic amphiphilic copolymer with solubilizing properties (Nagy et al., 2012). Xylitol (XYL) is freely water-soluble sugar alcohol (polyol) (Rowe et al., 2009). To date, there is only a little knowledge available about the use of XYL in a melt (co-fusion) method for fabricating SDs of drugs.

Since pharmaceutical SDs are virtually always used in a powder form, a deeper understanding of the particle properties (i.e., particle size and size distribution, shape, surface morphology, surface area) and bulk powder behavior (i.e., powder flow, moisture sorption, caking, wetting, dissolution) associated with such powders is of critical importance. To date, however, the studies dealing with the interactions of amorphous SD powders with air/water as well as the particle and bulk powder behavior of SDs are scarce. The particle size is a crucial characteristic of pharmaceutical powders influencing the dissolution of a poorly water-soluble drug. The powders with smaller particles have an increased surface area, and hence higher effective surface area for wetting and dissolution. **Particle properties also greatly influence bulk powder flow properties, which is important in both batch-wise or continuous pharmaceutical manufacturing processes (Van den Eynde et al., 2015).** Powder flow is of critical importance in e.g., tablet manufacturing (Emery et al., 2009), 3D printing (laser sintering) (Van den Eynde et al., 2015), and in formulating inhalable drug delivery systems (Mykhaylova et al., 2011). All limitations in bulk powder flow impair the mass and content uniformity of solid dosage forms.

The primary goals of the present study were (1) to investigate the particle properties and bulk powder behavior of the QC molten two-phase SDs of a poorly water-soluble drug (IND) with two different carrier materials (SOL and XYL), and (2) to elucidate the impact of these material properties on the formulation and performance of such SDs. A particular attention was paid to the effects of the matrix formers (amorphous hydrophilic polymer *vs*

crystalline sugar alcohol) and a QC melt (co-fusion) method on **the particle properties and bulk powder behavior of SDs.**

2. MATERIALS AND METHODS

2.1 Materials

The γ-polymorphic form of IND (γ-IND) (NLT 97.5%, Acros Organics, England) was used as a poorly water-soluble model drug. The α-polymorphic and amorphous forms of a model drug were prepared as described in our previous study (Semjonov et al., 2017). Soluplus® (BASF SE Pharma Ingredients & Services, Germany) was used as a solubilizing polymeric matrix former. Xylitol (Ph.Eur.) was used as a small-molecule freely soluble SD matrix former. Table 1 summarizes the physicochemical properties of IND and SD carrier materials.

2.2 Fabrication of SDs and physical binary mixtures (PMs)

Pure materials were manually sieved (150 µm) prior to further use and characterization. The preparation of the QC molten SDs and corresponding PMs has been presented in detailed elsewhere (Semjonov et al., 2017). Hence two-phase systems were obtained instead of molecularly dispersed SDs.

Table 1. Solid-state properties, molecular weight, melting point and bulk density of the materials used in the solid dispersions (SDs).

Material	Solid-state (particle shape)	Molecular weight (g/mol)	Melting point (Tm) / Glass transition (Tg)	Density (bulk) (g/cm^3)	Ref.
γ-IND	crystalline (rectangular)	357.79	160-161 °C (T_m)	1.37	(19)
α-IND	crystalline (needle)	357.79	152-154 °C (T_m)	1.42	(19)
Amorphous IND	amorphous	357.79	42 °C (T_g)	1.32	(20,21)
SOL	amorphous (round)	90,000-140,000	70 °C (T_g)	0.5-0.6	(22,23)
XYL	crystalline (oval)	152.15	92-96 °C (T_m)	0.8-0.85	(15)

Key: IND = indomethacin, SOL = Soluplus®, XYL = xylitol.

2.3 Moisture content analysis

Karl-Fischer (KF) titration (Mettler Toledo V30 Volumetric KF Titrator, Mettler-Toledo GmbH, Schwerzenbach, Switzerland) was used for determining the total water content of materials. The KF titrations (n = 2-3) were carried out at 21 °C temperature / 22% relative humidity (RH).

2.4 Contact angle measurements

Contact angle measurements (CAM200, ver. 4.1, KSV Instruments, Finland) were performed with the flat-faced compacts (m = 300 mg) prepared using a tabletop hydraulic press with a 13-mm die. Each compact was pressed using 100 MPa of pressure for 30 s. A purified water drop (MilliQ, EMD Millipore Corporation, Billerica, MA, USA) was used as the testing liquid. Images were taken within 40 ms after the liquid drop touched the surface of the compact, and both angles were recorded.

2.5 Moisture sorption

The moisture sorption of the drug, carrier materials, PMs and SDs was investigated by storing the pre-weighed samples (100 mg) on open petri dishes. The petri dishes were kept

at a constant temperature (25 °C) and RH 95% for 7 days. **All samples were kept at 30 °C for 24 h (0% RH) before the first weighing.** The moisture sorption was calculated from the weight gain using the following equation (Eq. 1) (Maddineni et al., 2015):

$$G = [(wf - wi)/S]\text{x } 100 \quad \text{(Eq. 1)}$$

where S is the initial mass of the sample, w_i is the total original mass of a petri dish and the sample, and w_f is the total end mass of a petri dish and the sample. Total three parallel determinations were made.

2.6 Scanning electron microscopy

Scanning electron microscope (SEM) (Zeiss EVO MA 15, Germany) was exploited for imaging the particle size, shape, surface porosity and morphology of the samples. The samples were attached on a carbon tape, and sputter coated with platinum (3-5 nm) in an argon atmosphere. The measurements were carried out under low vacuum. Martin's diameter of 50 randomly selected particles was determined in vertical direction from SEM images and particle size was measured by Image J (NIH, USA).

2.7 Powder flow test

The powder flow was determined using a novel in-house flow testing device (**Fig. 1**). The flow testing device has a sample cuvette mounted on a stepper motor, which was controlled with custom-made software. The cuvette consisted of two vertically positioned chambers separated by a 3 mm orifice. The powder was placed in the left chamber, and the cuvette was subjected to a specific acceleration profile, consisting of a slow acceleration and rapid deceleration when moving to the right and a rapid acceleration and slow deceleration when moving to the left. As a result of the acceleration profile and based on Newtonian mechanics, the powder is able to

gradually move to the opposite chamber through the orifice. When the powder was completely transferred to the opposite chamber, the measurement was terminated. The result was expressed as the amount of powder transferred per movement (mg/movement). The acceleration profile was programmed using MATLAB (The MathWorks, Inc., Natick, MA, USA). The testing method was validated with known excipients and against comparable powder flow measurements found in the literature (Seppälä et al., 2010).

Fig. 1. Schematic representation of the in-house powder flow measurement technique (not to scale). The powder is loaded in the left chamber, and based on Newtonian mechanics it is gradually transferred to the right chamber as a result of rapid acceleration while moving to the left and rapid deceleration while moving to the right.

2.8 Dissolution test in vitro

The dissolution tests were carried out using an USP paddle method (Distek Dissolution system 2100B, Distek, Inc., NJ, U.S.A). A table-top UV–VIS spectrophotometer (Specord 200 plus, AnalyticJena, Germany) was used at the analytical wavelength of 370 nm for the analysis of the PM and SD samples (n = 3). Prior to experiments, it was verified that neither SOL nor XYL showed any absorption at this specific wavelength. The two buffer solutions (Ph.Eur.), pH 1.2 and pH 6.8, were used as a dissolution medium at 37.0 ± 0.5 °C. **The total volume of the medium in each dissolution vessel was 500 ml and the amount of powder mass used for testing was 400 mg (100 mg for pure IND).** The rotation speed of the paddles was set at 100 rpm. At regular time intervals (10, 20, 30, 60, 360, and 1440 min), the samples of 5 ml were manually collected with a syringe and replaced accordingly with the pure buffer solution in a

dissolution vessel. The samples were filtered using a 25-mm syringe filter (VWR, USA) and through cellulose filters with a pore size of 45 µm. The first 2 ml of the filtrated solution was not included in the quantitative analysis with a UV-VIS spectrophotometer.

2.9 Data analysis

ImageJ (vers. 1.50i) was applied for measuring the particle size of samples, and a normality distribution was checked with a Shapiro-Wilk test. The mean values of particle size and drug release (% dissolved) were compared with a t-test. The statistical analysis ($p < 0.05$) of contact angle results was performed with a ANOVA one-way test and Tukey test.

3. RESULTS AND DISCUSSION

3.1 Particle properties

Virtually all critical pharmaceutical **bulk** powder properties, such as flowing, segregation, adhesion, water sorption and dissolution are dependent on the particle size, shape and surface morphology of the powder mixture (Mosharraf and Nyström, 1995). **Fig. 2** illustrates the SEM images of the particles representing the solid-state forms of IND (**2A-C**) and the two carrier materials studied (**2D, E**). The γ-form of IND displayed pointed and plate-like particles (**Fig. 2A1**), whereas the particles of α-IND were clearly needle-like in shape (**Fig. 2B2**). Amorphous IND and the carrier materials SOL and XYL possessed larger agglomerates or particles with an uneven shape and size (**Figs 2C1, D1, E2**). SOL had the largest particles ranging from 100 to 200 µm in diameter, and γ-IND the smallest ones with a size range below 50 µm. The PMs showed

clearly distinguishable γ-IND particles and larger carrier particles (**Figs 3A1, B1**). Interestingly, the larger particles in the PMs of γ-IND and XYL was layered with tiny drug particles (**Figs 3B1,2**).

The SDs with SOL showed oval shaped fused particles or agglomerates (**Fig. 3A2**). The SDs of IND and XYL possessed much larger particles with a rough surface coming from the surface recrystallization of XYL (**Fig. 3B2**). It is obvious that the topographical differences between the SDs consisting of different carrier materials are due to the differences in material properties. Palomäki et al. (2016) showed that amorphous XYL recrystallizes within five minutes at a room temperature (RT). Taking into consideration this fast XYL recrystallization tendency and the fact that the sample was ground after QC melting, the present XYL containing SDs are crystalline. The crystalline state of such SDs was confirmed in our previous study with X-ray powder diffraction complemented with FTIR spectroscopy (Semjonov et al., 2017).

Fig. 2. SEM micrographs of pure materials. Keys: A1/A2 – -IND; B1/B2 – -IND; C1/C2 – amorphous IND; D1/D2 – SOL; E1/E2 – XYL; IND = indomethacin; SOL = Soluplus®; XYL = xylitol. Magnification: ×100 and ×500.

Fig. 3. SEM micrographs of physical mixtures (PMs) and quench cooled (QC) molten solid dispersions (SDs). Key: A1 – PMs of -IND and SOL (1:3); A2 – SDs of IND and SOL (1:3); B1

– PMs of -IND and XYL (1:3); B2 – SDs of IND and XYL (1:3). IND = indomethacin; SOL = Soluplus®; XYL = xylitol. Magnification: ×500. **Drug particles are indicated by arrows.**

According to the Shapiro-Wilk test, the particle size of the present samples measured with SEM did not follow a normal distribution ($\alpha = 0.05$) (the particle size distributions are shown in **Fig. 4**). The difference between the particle size of PMs and respective SDs was statistically significant with both SOL and XYL carrier materials ($p < 0.05$). However, the statistical analysis did not show any significant difference between the particle size of SDs with SOL and XYL.

Fig. 4. Particle size distribution (n=50) of (a) γ- IND, (b) amorphous IND, (c) SOL, (d) XYL, (e) solid dispersion (SD) of IND and XYL, (f) physical mixture (PM) of IND and XYL, (g) PM of IND and SOL, (h) SD of IND and SOL. Keys: IND-indomethacin; SOL-Soluplus®; XYL-Xylitol.

3.2 Residual water content

The moisture content and wetting of pharmaceutical powders can essentially affect the bulk powder behavior, manufacturing, performance and stability of a final pharmaceutical dosage form. **Fig. 5** shows the residual water content of pure materials, PMs and SDs. The water contents for pure materials were 0.24%, 2.49 (SOL) and 0.42% (XYL), and these results are in line with the values presented in the literature (Priemel et al., 2013). The hydrophobic IND had a low water content, and this was verified also in the moisture sorption studies. SOL is an amorphous polymer known to be able to absorb water vapor from the environment, and the polymer chains most likely interact more readily with water compared to XYL molecule (crystalline material). XYL is a small-molecule nonporous sugar alcohol, and it possesses much

lower water content due to its crystalline structure. Different polymers behave differently, and the water may exist in different states within the material-bound vs free water which also affects the behavior of polymers in the presence of drug molecules (Williams et al., 2013).

As shown in **Fig. 5**, the differences in the water content of PMs and SDs consisting of either SOL or XYL, are evident. With the PMs of γ-IND and SOL, the water content increased as the amount of polymer was increased (**Fig. 5**). With the PMs of γ-IND and XYL, the water content was virtually independent of the amount of the carrier used (**Fig. 5**). The moisture content of the SDs of IND and SOL (1:3) was smaller than that observed with the respective PMs. Most likely this is due to the fact that within the glassy suspension of IND and SOL, the hydrogen (H) bonding between the drug and polymer reduces the potential of H-bonding of the water to either component. With the SDs of IND and XYL (1:3), the moisture content was higher (0.52%) compared to that of PMs (0.35%). This small difference in water content could be explained by the more hygroscopic nature of amorphous IND dispersed in a crystalline hydrophilic XYL matrix in two-phase SDs (amorphous precipitation system). Since the surface of the PMs and SDs of IND and XYL samples was covered with drug particles (confirmed by SEM, **Fig. 3**), the adsorption of water on crystalline XYL most likely largely depended on the solid state of the drug. Moisture absorption of all samples in bulk was measured to confirm these results.

Fig. 5. Water content (w/w %) of pure materials (γ-IND, SOL, XYL), physical mixtures (PMs), and quench cooled (QC) molten solid dispersions (SDs) (n = 3). Key: IND = indomethacin; SOL = Soluplus®; XYL = xylitol. The symbol (*) indicates the statistical significant difference ($p < 0.05$).

3.3 Moisture sorption analysis

The results of moisture sorption analysis are shown in **Fig. 6**. As expected, amorphous IND was found to be more hygroscopic (1.3-2% increase in weight gain) than γ-IND. The corresponding increase in weight gain for SOL and XYL was 13-18% and 34-89%, respectively. The pure materials were exposed to high 95% RH for 7 days, but the equilibrium was reached already within 96 hours, with an exception of XYL which continued to rapidly absorb moisture for up to 144 hours (89%).

The PMs of IND and SOL (1:3) exhibited slightly higher values for weight gain (water vapor sorption) compared to the respective SDs. This result is in line with the water content measurement results. The moisture sorption of SDs of IND and SOL (1:3) was much higher compared to that of pure IND forms (γ, α, amorphous IND). Most likely, the inclusion of SOL between IND molecules in regions of molecular-level mixing makes the interior of the SD particles more hygroscopic, thus resulting in increased water vapor uptake compared to pure forms.

As seen in **Fig. 6**, the SDs of IND and XYL (1:3) showed a similar weight gain (water vapor sorption) as its respective PMs. Rapid changes in the weight gain of both PM and SD samples occurred within the first 24 hours (25.2-35.5% increase in weight gain). The SDs of IND and XYL (1:3) dissolved partially in sorbed water and formed transparent droplets. According to the literature, the water sorption of sugars ranges typically 3-5 mg/g, and water activity (a_w) of XYL is 0.6 (25 °C) (Weisser et al., 1982). At the a_w levels of 0.6-0.7, water molecules are

adsorbed on the crystal surface, but at the a_w values higher than 0.7, amount of absorbed water rises steadily resulting in the dissolution of the crystals (Demertzis et al., 1989). As IND and XYL were in two separate phases in both SDs and PMs, the overall effect of the hydrophobic small molecule on the moisture sorption was negligible.

In summary, the PMs and SDs of IND with XYL can sorb water vapor more readily compared to the corresponding PMs and SDs of IND with SOL. The lower weight gain (water vapor sorption) of SOL containing samples suggests a strong H-bonding formation between drug and polymer, which supports also our previous study (Semjonov et al., 2017). According to the literature, water entrapped in the amorphous SD structure can greatly influence the critical attributes (i.e., performance and stability) of the system (Brough and Williams, 2013). Puncochova and co-workers (2014) reported that the water sorption of SOL stored at 90% RH resulted in a 25% mass gain. In their study, the PMs and SDs of valsartan and SOL (1:3) were subjected to dynamic water sorption (0-95% RH). Interestingly, both PMs and SDs (the latter assumed to include molecular-level mixing) showed identical sorption isotherms with approximately 16% of a mass gain, which is in line with our findings. The reason for such phenomenon is obviously strong drug-polymer interactions and the blockage of H-bonding functional groups for water sorption. Nevertheless, the SDs showed faster dissolution (pH 6.8) kinetics than respective PMs (Puncochova et al., 2014).

Fig. 6. Moisture sorption of pure materials (γ-IND, SOL, XYL), physical mixtures (PMs) and quench cooled (QC) molten solid dispersions (SDs) (n = 3). Key: IND = indomethacin; SOL = Soluplus®; XYL = xylitol.

3.4 Wetting properties

No statistically significant differences between the contact angle values of γ-IND (51.9° ± 16.6°), α-IND (63.8° ± 8.4°), and amorphous IND (54.9° ± 4.5°) were found (**Fig. 7**). The contact angle value for γ-IND (51.6°) obtained in our study was slightly smaller than that (76°) reported in the literature (Defilippis et al., 1991). XYL showed higher wettability than SOL with the contact angle values of 18.3° ± 2.5° and 76.2° ± 5.8°, respectively. SOL has been investigated as a means for improving the wettability of powders (Sakurai et al., 2017). XYL is known to have a low contact angle and exhibits good hydrating properties (Bruggeman et al., 2010). However, the contact angle values obtained for the PMs of IND and XYL (58.6° ± 14.3°) were similar to those obtained for the PMs of IND and SOL (70.3° ± 6.6). Relatively high contact angles compared to pure XYL were probably due to the poor miscibility of the components, thus resulting in the disposition of γ-IND particles on the carrier surface. Even though the difference was not statistically significant, the trend can be still observed.

The contact angle values for the SDs containing different carrier material were 54.9° ± 8.0 (IND and SOL 1:3) and 46.4° ± 5.7 (IND and XYL 1:3). The difference in contact angle values, however, was not statistically significant. It is evident that amorphous IND in the SDs absorbs water more readily compared to crystalline γ- and α-IND (supported with moisture absorption results, **Fig. 7**), thus resulting in decreased and more uniform contact angle values obtained with the SDs with different carrier materials. With the SDs containing XYL, the increase in wettability was obviously due to the hydrophilic nature of XYL present in samples. The hydrophobic nature of poorly-water soluble drugs is expressed in contact angle values below 90° (piroxicam

anhydrate forms and monohydrate values of 73-75°, nifedipine 85°, carbamazepine dihydrate 61°) (Chutimaworapan et al. 2000; Vrečer et al., 2003; Tian et al., 2007). Formulating the drug in PMs and SDs usually results in improved wettability, which is correlated with the improved intrinsic dissolution rate of the model drug (Chokshi et al., 2007). However, according to Defilippis et al. (1991), the formulation of IND in the SDs with Eudragit E® (1:1) did not improve the wettability of IND (contact angle value 72°). The amount of drug dispersed on the surface of the system has been shown to affect a contact angle level (Dahlberg et al., 2008), and this could also explain the improved wettability of PMs and SDs observed in our study.

Fig. 7. Contact angle of pure materials (γ-IND, α-IND, amorphous IND, SOL, XYL), physical mixtures (PMs) and quench cooled (QC) molten SDs (n = 3). Key: IND = indomethacin; SOL = Soluplus®; XYL = xylitol.

3.5 Powder flow

To date, very little is known on the bulk powder flow properties of the QC molten SDs of the drug and carrier materials. In our study, the powder flow was evaluated using an in-house automated cuvette rheometer designed for testing in a small scale (**Fig. 1**). **Fig. 8** shows the dependence of the number of cuvette movements and the sample mass in the chambers, thus quantifying the powder flow rate (mg/movement) of the sample. As expected, the powder flow of pure γ-IND was very poor due to the morphology and size of particles (rectangular, sharp edged particles). Both carrier materials (SOL/XYL) presented free flowing powder behavior. Similar results have been shown previously (Seppälä et al., 2010; Reginald-Opara et al., 2015).

As the amount of the carrier material was increased, the powder flow of the PMs significantly improved (**Fig. 8**). The PMs of γ-IND and SOL with the highest drug-polymer ratio (1:9) showed the highest powder flow rate (21.2 mg / movement), while the powder flow rate of the PMs (3:1) was the poorest (6.0 mg / movement) (**Fig. 8A**). Similar results were obtained with the PMs of γ-IND and XYL. The 1:9 PMs (drug-sugar alcohol ratio) showed a good powder flow (20.0 mg / movement) and 3:1 PMs very poor powder flow (6.2 mg / movement) (**Fig. 8B**). It is well known that sugars with a low water activity possess good powder flow properties (Seppälä et al., 2010). According to the literature, some established polymeric carriers (polyvinyl pyrrolidone, hydroxypropyl methylcellulose, chitosan) can advance the powder flow of crystalline IND in PMs (Yadav and Yadav, 2016). The powder flow of IND in these PMs was evidently improved due to contact (drug particles) with round shaped polymeric/non-polymeric carriers. Li et al. (2015) reported that the powder flow properties of paracetamol in PMs with SOL was improved since the drug crystals formed a thin coating layer on the surface of the polymer (SOL) particles.

The powder flow of the SDs of IND and SOL was superior compared to that of the corresponding PMs with the powder flow rate values of 17.6 mg /movement and 12.9 mg / movement, respectively (**Fig. 8**). This could be explained by the larger average particle size and more spherical shape (oval) of the SDs compared to that of PMs (**Fig. 3 and Fig. 4**). Djuris et al. (2013) showed that the SDs of SOL advanced the powder flow properties of carbamazepine (Djuris et al., 2013). Dabbagh and Taghipour (2007) reported that the SDs of ibuprofen and PEG have superior powder flow properties over the corresponding PMs, and the authors suggested that SDs can be used for promoting the bulk powder flow of the drug. In our study, the moisture content of the SDs (SOL) was somewhat smaller than that observed with the respective PMs (**Fig.**

5). Nevertheless, it is evident, that the difference in particle size and morphology is the major factor leading to the differences in the powder flow of SDs and PMs.

The powder flow properties of the SDs of IND and XYL (1:3), and the corresponding PMs were very similar (**Fig. 8**). This could be explained by the crystallization of XYL from the SDs resulting in the SD bulk powder with similar properties as PMs. The water content of the samples showed only small differences and moisture sorption was also alike. Indeed, the particles of the SDs were larger compared to those of the PMs, but the adhesion of IND particles to the surface of XYL particles in the PMs unified the surface roughness of the PM and SD particles. The particles with smooth surfaces were observed with both PMs (XYL) and SDs (XYL) (as shown in **Fig. 3**) which could explain their similar flow properties. According to the literature, the adhesion and friction forces between the drug and carrier material are greatly dependent on the surface roughness of the particles (Podczeck, 1998). Genina and co-workers (2009) revealed that the particle surface engineering with ultrasonic water mist improved the powder flow of lactose due to particle surface smoothing and loss of fines.

Fig. 8. Powder flow of pure materials (γ-IND, SOL, XYL), physical mixtures (PMs) and quench cooled (QC) molten SDs (n = 3). Key: IND = indomethacin; SOL = Soluplus®; XYL = xylitol. (A) PMs and SDs with SOL; (B) PMs and SDs with XYL. Reference materials for a powder flow test: Lactose 80M – 31.72 ± 1.31 mg/movement (= good flowability), Lactose 200M – 8.37 ± 0.27 mg/movement (= poor flowability) (dotted lines).

In summary, the inclusion of SOL or XYL in the PMs and SDs clearly promotes the powder flow of poorly flowing IND. We found that the bulk powder flow properties of both PMs and SDs were directly related to the amount of carrier polymer used, and the SDs of the drug and

carrier material presented equal powder flow as the corresponding PMs. In the PMs and SDs with XYL, drug particles were adhered or fused onto the surface of XYL, which unified also the powder flow of these systems. Moisture sorption most probably does not play any significant role in such systems, since XYL does not absorb much water below 80% RH (Rowe et al., 2009).

3.6 Dissolution

The Biopharmaceutics Classification System (BCS) deploys IND among the class II drugs which are characterized by slow or partial dissolution and fast absorption *in vivo* (Amidon et al., 1995). Accordingly, with the present drugs dissolution is a critical attribute governing their oral bioavailability and therapeutic effect. Craig (2002) reported that the drug-loaded SDs can present primarily (1) the carrier-controlled dissolution (especially at low drug loadings), or (2) drug-dependent dissolution. The prevalence of the release mechanism is dependent on the miscibility and solubility of the components in the concentrated solution of the polymer (Craig, 2002). In addition, several processes competing with one another take place simultaneously during the dissolution of SDs, and both the drug and carrier polymer properties affect the total drug release (Kogermann et al., 2013).

As seen in **Fig. 9A**, the percentage of γ-IND dissolved within 30 min was 35.8 ± 2.6% in a pH 6.8 phosphate buffer solution at 37 °C. This shows significantly slower drug dissolution compared to that of α-IND. The percentage of amorphous IND and α-IND dissolution at 30 min was 67.7 ± 9.1% and 63.5 ± 2.4%, respectively (**Fig. 9A**). Within 360 min, more than 90% of γ-, α-IND and amorphous IND was dissolved. No statistically significant differences in wettability were found between the two IND polymorphs and an amorphous form (as shown in **Fig. 9**). A clear difference in the dissolution rate, however, was observed. Both amorphous IND and α-IND

showed higher extent and rate of dissolution within the first 10 min compared to γ-IND (the amount of drug dissolved was 47.4 ± 6.2%, 44.3 ± 5.2% and 7.1 ± 0.6%, respectively).

The SDs of IND and SOL form a two-phase glassy suspension where the amorphous IND is thoroughly mixed with amorphous SOL (Semjonov et al., 2017). **Fig. 9A** shows that the initial drug release from the SDs of IND with SOL at 10 min was clearly higher (72.0 ± 0.7%) compared to that of the corresponding PMs (11.7 ± 1.7%), although the smaller particle size should have favored the PM. As shown, the SDs had also significantly improved wettability over the corresponding PMs (**Fig. 6**). This enhanced dissolution is obviously as a result of improved wetting of IND and inhibited crystallization of the drug from amorphous form or from solution to α form by SOL. Over 85% of the drug was released from the SDs of IND and SOL within 6 h (360 min) of the dissolution test (**Fig. 9A**). It is known that molecular mixing between IND and SOL in one-phase SD completely inhibited drug release (Surwase et al., 2015). The release of IND from the corresponding PMs within the first 10 min was close to that obtained with pure γ-IND at pH 6.8 (11.8 ± 1.7% and 7.1 ± 0.6%). The low release rate is related to very poor wettability of PMs and γ-IND (**Fig. 9**), and the formation of polymer (SOL) gel upon wetting. Since γ-IND is hydrophobic, the **amphiphilic** SOL molecules tend to adhere to IND crystals, thus decreasing the effective dissolution surface area. **The present results are consistent with earlier studies showing that the PMs of IND and SOL exhibit a slower dissolution rate because of the gel formation and strong H-bonding (Terife et al., 2012).**

According to our recent study, the SDs of IND and XYL are two-phase systems in which IND is in amorphous form in a crystalline XYL matrix (Semjonov et al., 2017). As seen in **Fig. 9B**, the PMs of IND and XYL (1:3) showed much higher initial dissolution rate at 10 min compared to that of γ- IND (50.9 ± 0.2% and 7.1 ± 0.6%, respectively). The present PMs (unlike the PMs of IND and SOL) do not have any swelling properties, which could hinder the drug

dissolution supported by absorption and wetting studies (**Fig. 6 and 7**) The difference in drug release of the SDs of IND and XYL (1:3) after 10 min was not statistically significant compared to the corresponding PMs (**Fig. 9B**). At 30 min, the difference in the dissolution between the PMs and SDs was even more pronounced (76.3 ± 3.1% and 63.9 ± 2.9%, respectively). The drug release was improved with XYL containing PMs and SDs (**Fig. 9B**) without reaching plateau as with SOL SDs. Excipient intrinsic properties are of critical importance in enhancing the solubility and dissolution rate of poorly water-soluble drugs. Most likely on the course of rapid dissolution of XYL, the IND particles did not adhere to each other and higher effective surface area was achieved. XYL as a carrier material is freely water-soluble polyalcohol with no gel forming ability (Rowe et al., 2009). **As expected, the drug release studies in acidic environment (pH 1.2) showed very limited dissolution of PMs and SDs (Fig. 9).**

Fig. 9. *In-vitro* dissolution profiles of pure materials (γ-IND, α-IND, amorphous IND), physical mixtures (PMs) and quench cooled (QC) molten solid dispersions (SDs) (n = 3). Key: IND = indomethacin; SOL = Soluplus®; XYL = xylitol. The dissolution medium was a pH 6.8 phosphate buffer solution (37 °C).

3.7 Comparison of the dissolution behavior of two-phase QC SDs

We found that the dissolution behavior of SOL and XYL systems are affected by carrier specific characteristics and solid state form of the drug. Strong H-bonds between the drug and SOL hindered drug release from PMs, unlike with XYL PMs. The plateau effect detected with

SOL SDs was not the case with XYL SDs, as drug released steadily up to 360 min. Even though, the initial dissolution rate was faster for SOL SDs, but overall increased amount of drug was released with XYL SDs.

4. CONCLUSION

The QC molten two-phase SDs of a poorly water-soluble drug (IND) with two different matrix formers (amorphous copolymer *vs* crystalline sugar alcohol) exhibit significant differences in particle properties and bulk powder behavior. The water content of the QC molten SDs can vary depending on the type and solid-state form of the carrier material as well as the intrinsic hydrophilic/hydrophobic nature of the materials. Both carrier materials studied here can advance the powder flow properties of a cohesive IND powder, and this improvement is directly related to the amount of a carrier material used in PMs or SDs. The inclusion of a carrier material (SOL/XYL) in both PMs and SDs improves also the wetting properties of an IND powder, where XYL mixtures showed higher moisture sorption compared to SOL ones. The *in-vitro* drug release of the present SDs and PMs has a carrier-controlled release mechanism at pH 6.8. The hydrophilic nature of carriers mitigated the hydrophobic properties of the drug and improved its release. **SOL in the PMs can hinder the drug dissolution via polymer gel formation.** The enhanced drug dissolution from the SDs with SOL is due to improved wetting and inhibited crystallization of IND. XYL as a freely water-soluble polyalcohol advances the solubility and dissolution of IND most likely through better wetting properties and hydrophilic environment in the solution.

CONFLICT OF INTEREST

The Authors declare no conflicts of interest.

ACKNOWLEDGEMENTS

MSc Jukka Saarinen is acknowledged for the help with contact angle measurements. MSc Tuomas Saarinen, MSc Juuso Paloranta and MSc Lassi Seppälä are acknowledged for conducting powder flow tests. Prof. Kalle Kirsimäe and Marian Külaviir are thanked for performing the SEM experiments.

FUNDING

The work is part of the Estonian national PUT 1088 and IUT-34-18 projects.

REFERENCES

1. Sekiguchi K, Obi N. Studies on absorption of eutectic mixture. I. A comparison of the behavior of eutectic mixture of sulfathiazole and that of ordinary sulfathiazole in man. Chem Pharm Bull. 1961;9(11):866-72.
2. Vasconcelos T, Sarmento B, Costa P. Solid dispersions as strategy to improve oral bioavailability of poor water soluble drugs. Drug Discov Today. 2007;12(23-24):1068-75.
3. Williams HD, Trevaskis NL, Charman SA, Shanker RM, Charman WN, Pouton CW, Porter CJH. Strategies to address low drug solubility in discovery and development. Pharmacol Rev. 2013;65(1):315-499.
4. Leuner C, Dressman J. Improving drug solubility for oral delivery using solid dispersions. Eur J Pharm Biopharm. 2000;50(1):47-60.
5. Brough C, Williams RO. Amorphous solid dispersions and nano-crystal technologies for poorly water-soluble drug delivery. Int J Pharm. 2013;453(1):157-66.

6. Surwase SA, Itkonen L, Aaltonen J, Saville D, Rades T, Peltonen L, *et al.* Polymer incorporation method affects the physical stability of amorphous indomethacin in aqueous suspension. Eur J Pharm Biopharm. 2015;96:32-43.

7. Thommes M, Ely DR, Carvajal MT, Pinal R. Improvement of the dissolution rate of poorly soluble drugs by solid crystal suspensions. Mol Pharm. 2011;8(3):727-35.

8. Thommes M. Featured Article. APV Drug Deliv Focus Gr Newsl – 1/2012. 2012;23(1):3-4.

9. Xie Y, Xie P, Song X, Tang X, Song H. Preparation of esomeprazole zinc solid dispersion and study on its pharmacokinetics. Int J Pharm. 2008;360(1-2):53-7.

10. DiNunzio JC, Brough C, Miller DA, Williams RO, McGinity JW. Fusion processing of itraconazole solid dispersions by kinetsol® dispersing: A comparative study to hot melt extrusion. J Pharm Sci. 2010;99(3):1239-53.

11. Newman A, Knipp G, Zografi G. Assessing the performance of amorphous solid dispersions. J Pharm Sci. 2012;101(4):1355-77.

12. Semjonov K, Kogermann K, Laidmäe I, Antikainen O, Strachan CJ, Ehlers H, *et al.* The formation and physical stability of two-phase solid dispersion systems of indomethacin in supercooled molten mixtures with different matrix formers. Eur J Pharm Sci. 2017;97:237-46.

13. Janssens S, Van den Mooter G. Review: physical chemistry of solid dispersions. J Pharm Pharmacol. 2009;61(12):1571-86.

14. Nagy ZK, Balogh A, Vajna B, Farkas A, Patyi G, Kramarics Á, *et al.* Comparison of electrospun and extruded Soluplus®-based solid dosage forms of improved dissolution. J Pharm Sci. 2012;101(1):322-32.

15. Rowe RC, Sheskey PJ, Quinn ME. Handbook of pharmaceutical excipients. 6th ed. London: Pharmaceutical Press and the American Pharmacists Association; 2009.

16. Van den Eynde M, Verbelen L, Van Puyvelde P. Assessing polymer powder flow for the application of laser sintering. Powder Technol. 2015;286:151-5.

17. Emery E, Oliver J, Pugsley T, Sharma J, Zhou J. Flowability of moist pharmaceutical powders. Powder Technol. 2009;189(3):409-15.

18. Mykhaylova V, Dresely K, Klar F, Urbanetz NA. Carrier-free formulation of dry powder inhalates nanoparticle coating of drug microparticles. Pharm Ind. 2011;73(7):1324-31.

19. Chen X, Morris KR, Griesser UJ, Byrn SR, Stowell JG. Reactivity differences of indomethacin solid forms with ammonia gas. J Am Chem Soc. 2012;124(50):15012-9.

20. Xiang T-X, Anderson BD. Molecular dynamics simulation of amorphous indomethacin. Mol Pharm. 2013;10(1):102-14.

21. Andronis V, Zografi G. Crystal nucleation and growth of indomethacin polymorphs from the amorphous state. J Non Cryst Solids. 2000;271(3):236-48.

22. BASF. 2010. Soluplus® - Technical information. 2012;1-201.

23. Park F, Dust C, Dust C. Safety data sheet product identifier used on the label Soluplus®. 2017;(1):1-9.

24. Maddineni S, Battu SK, Morott J, Majumdar S, Murthy SN, Repka MA. Influence of process and formation parameters on dissolution and stability characteristics of Kollidon® VA 64 hot-melt extrudates. AAPS PharmSciTech. 2015;16(2):444-54.

25. Seppälä K, Heinämäki J, Hatara J, Seppälä L, Yliruusi J. Development of a new method to get a reliable powder flow characteristics using only 1 to 2 g of powder. AAPS PharmSciTech. 2010;11(1):402-8.

26. Mosharraf M, Nyström C. The effect of particle size and shape on the surface specific dissolution rate of microsized practically insoluble drugs. Int J Pharm. 1995;122(1-2):35-47.

27. Palomäki E, Ahvenainen P, Ehlers H, Svedström K, Huotari S, Yliruusi J. Monitoring the recrystallisation of amorphous xylitol using Raman spectroscopy and wide-angle X-ray scattering. Int J Pharm 2016;508(1-2):71-82.

28. Priemel P, Laitinen R, Barthold S, Grohganz H, Lehto VP, Rades T, *et al.* Inhibition of surface crystallisation of amorphous indomethacin particles in physical drug-polymer mixtures. Int J Pharm. 2013;456(2):301-6.

29. Weisser H, Weber J, Loncin M. Water vapour sorption isotherms of sugar substitutes in the temperature range 25 to 80 °C. Int Zeitschrift für Leb und Verfahrenstechnik. 1982;33:89-97.

30. Demertzis PG, Riganakos KA, Kontominas MG. Water sorption isotherms of crystalline raffinose by inverse gas chromatography. Int J Food Sci Technol. 1989;24(6):629-36.

31. Punčochová K, Heng JYY, Beránek J, Štěpánek F. Investigation of drug-polymer interaction in solid dispersions by vapour sorption methods. Int J Pharm. 2014;469(1):159-67.

32. Defilippis P, Boscolo M, Gibellini M, Rupena P, Rubessa F, Moneghini M. The release rate of indomethacin from solid dispersions with Eudragit E®. Drug Dev Ind Pharm. 1991;17:2017-28.

33. Sakurai Y, Mise R, Kimura S, Noguchi S, Iwao Y, Itai S. Novel method for improving the water dispersibility and flowability of fine green tea powder using a fluidized bed granulator. J Food Eng. 2017;206:118-24.

34. Bruggeman JP, Bettinger CJ, Langer R. Biodegradable xylitol-based elastomers: In vivo behavior and biocompatibility. J Biomed Mater Res Part A. 2010;95A(1):92-104.

35. Vrečer F, Vrbinc M, Meden A. Characterization of piroxicam crystal modifications. Int J Pharm. 2003;256(1-2):3-15.

36. Chutimaworapan S, Ritthidej GC, Yonemochi E, Oguchi T, Yamamoto K. Effect of water-soluble carriers on dissolution characteristics of nifedipine solid dispersions. Drug Dev Ind Pharm. 2000;26(11):1141-50.

37. Tian F, Sandler N, Aaltonen J, Lang C, Saville DJ, Gordon KC, *et al.* Influence of polymorphic form, morphology, and excipient interactions on the dissolution of carbamazepine compacts. J Pharm Sci. 2007;96(3):584-94.

38. Chokshi RJ, Zia H, Sandhu HK, Shah NH, Malick WA. Improving the dissolution rate of poorly water soluble drug by solid dispersion and solid solution–pros and cons. Drug Deliv. 2007;14(1):33-45.

39. Dahlberg C, Millqvist-Fureby A, Schuleit M. Surface composition and contact angle relationships for differently prepared solid dispersions. Eur J Pharm Biopharm. 2008;70(2):478-85.

40. Reginald-Opara JN, Attama A, Ofokansi K, Umeyor C, Kenechukwu F. Molecular interaction between glimepiride and Soluplus®-PEG 4000 hybrid based solid dispersions: Characterisation and anti-diabetic studies. Int J Pharm. 2015;496(2):741-50.

41. Dabbagh MA, Taghipour B. Investigation of solid dispersion technique in improvement of physicochemical characteristics of ibuprofen powder. Iranian J Pharm Sci. 2007;3:69-76.

42. Podczeck F. Adhesion forces in interactive powder mixtures of a micronized drug and carrier particles of various particle size distributions. J Adhes Sci Technol. 1998;12(12):1323-39.

43. Genina N, Räikkönen H, Heinämäki J, Antikainen O, Siiriä S, Veski P, *et al.* Effective modification of particle surface properties using ultrasonic water mist. AAPS PharmSciTech. 2009;10(1):282-8.

44. Djuris J, Nikolakakis I, Ibric S, Djuric Z, Kachrimanis K. Preparation of carbamazepine-Soluplus® solid dispersions by hot-melt extrusion, and prediction of drug-polymer miscibility by thermodynamic model fitting. Eur J Pharm Biopharm. 2013;84(1):228-37.

45. Li M, Gogos CG, Ioannidis N. Improving the API dissolution rate during pharmaceutical hot-melt extrusion I: Effect of the API particle size, and the co-rotating, twin-screw extruder screw configuration on the API dissolution rate. Int J Pharm. 2015;478(1):103-12.

46. Yadav VB, Yadav AV. Enhancement of solubility and dissolution rate of indomethacin with different polymers by compaction process. Int J ChemTech Res. 2009;1(4):1072-8.

47. Amidon GL, Lennernäs H, Shah VP, Crison JR. A theoretical basis for a biopharmaceutic drug classification: The correlation of in vitro drug product dissolution and in vivo bioavailability. Pharm Res. 1995;12(3):413-20.

48. Craig DQ. The mechanisms of drug release from solid dispersions in water-soluble polymers. Int J Pharm. 2002;231(2):131-44.

49. Kogermann K, Penkina A, Predbannikova K, Jeeger K, Veski P, Rantanen J, et al. Dissolution testing of amorphous solid dispersions. Int J Pharm. 2013;444(1-2):40-6.

50. Terife G, Wang P, Faridi N, Gogos CG. Hot melt mixing and foaming of Soluplus® and indomethacin. Polym Eng Sci. 2012;52(8):1629-39.

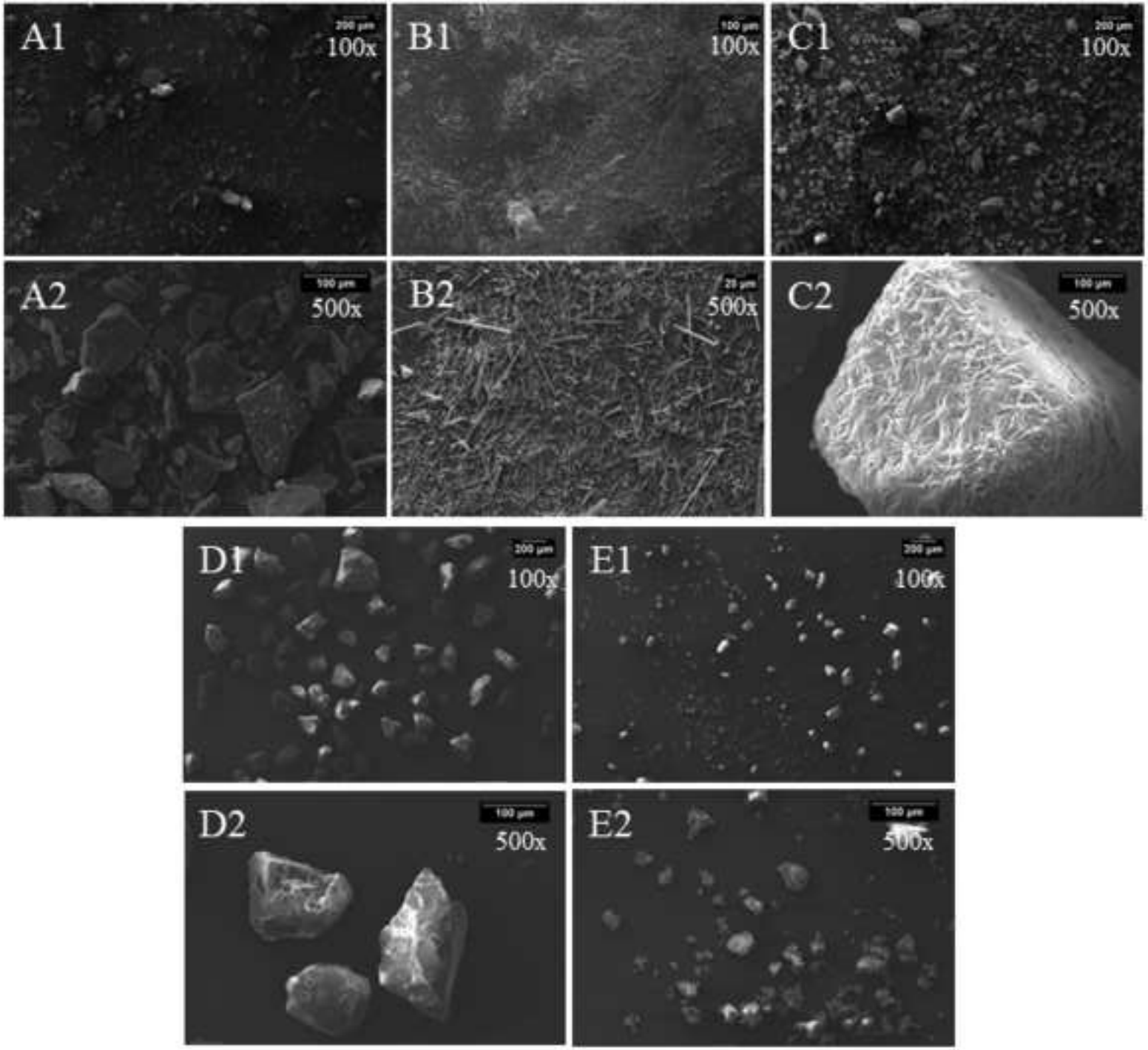

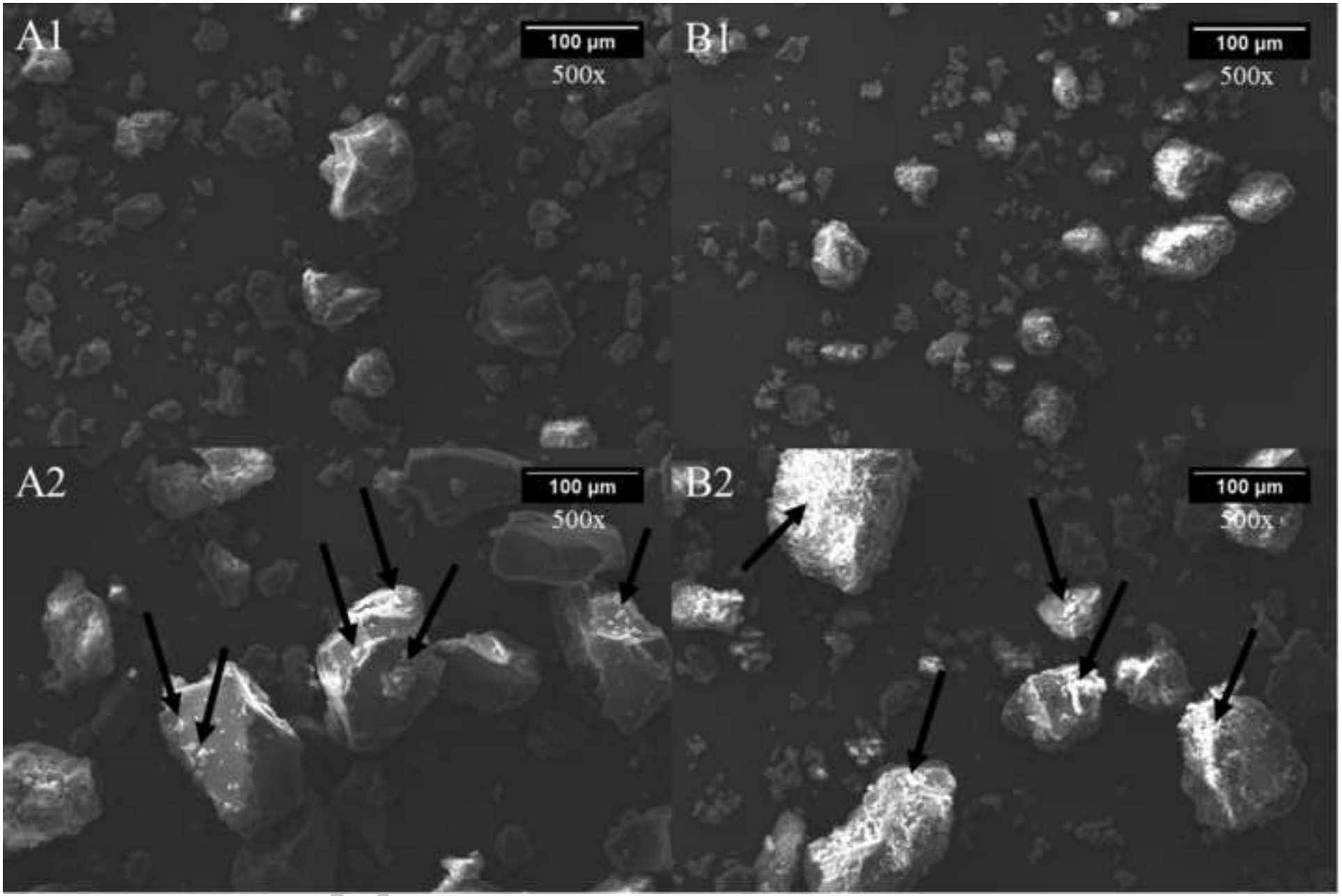

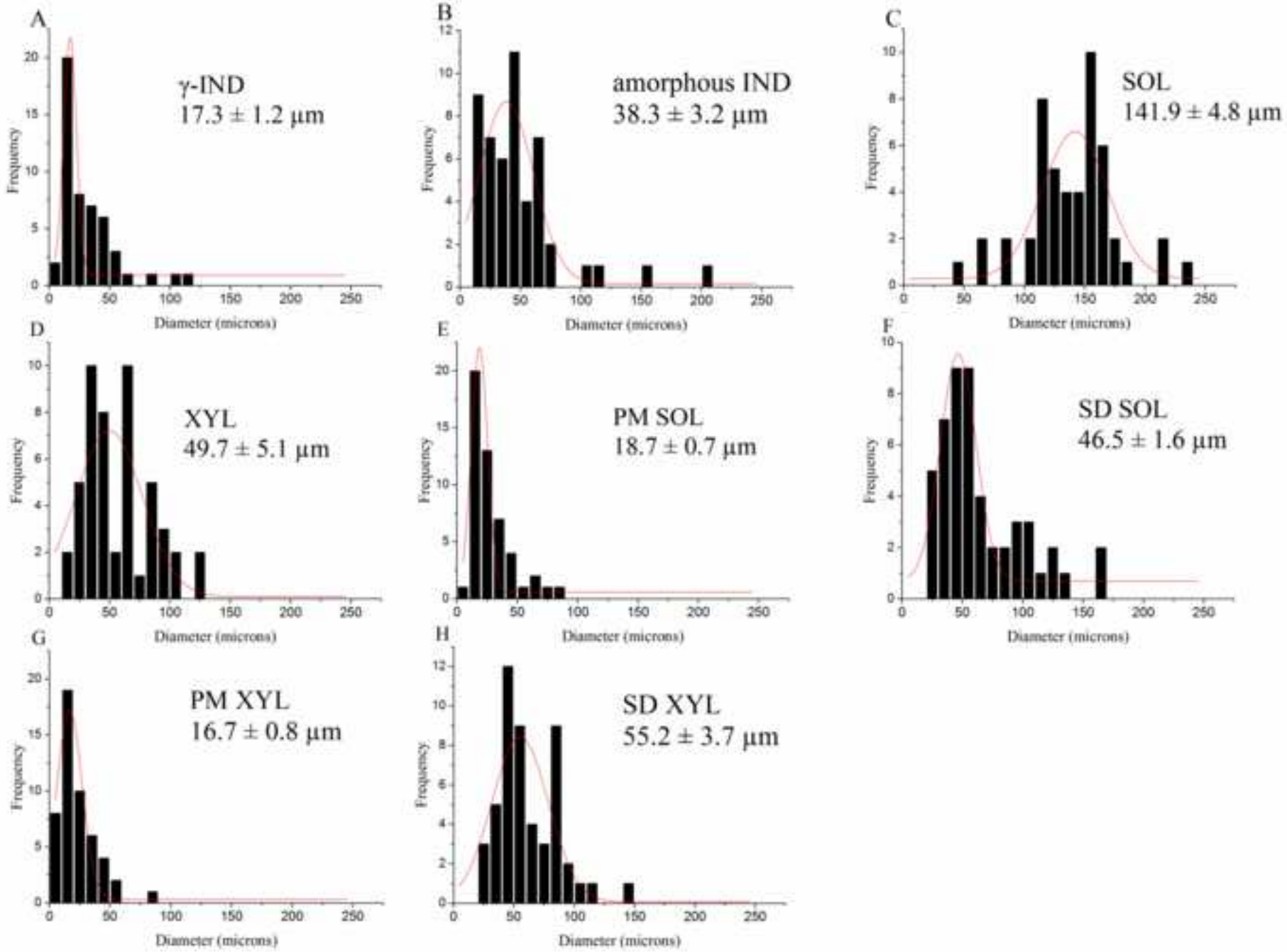

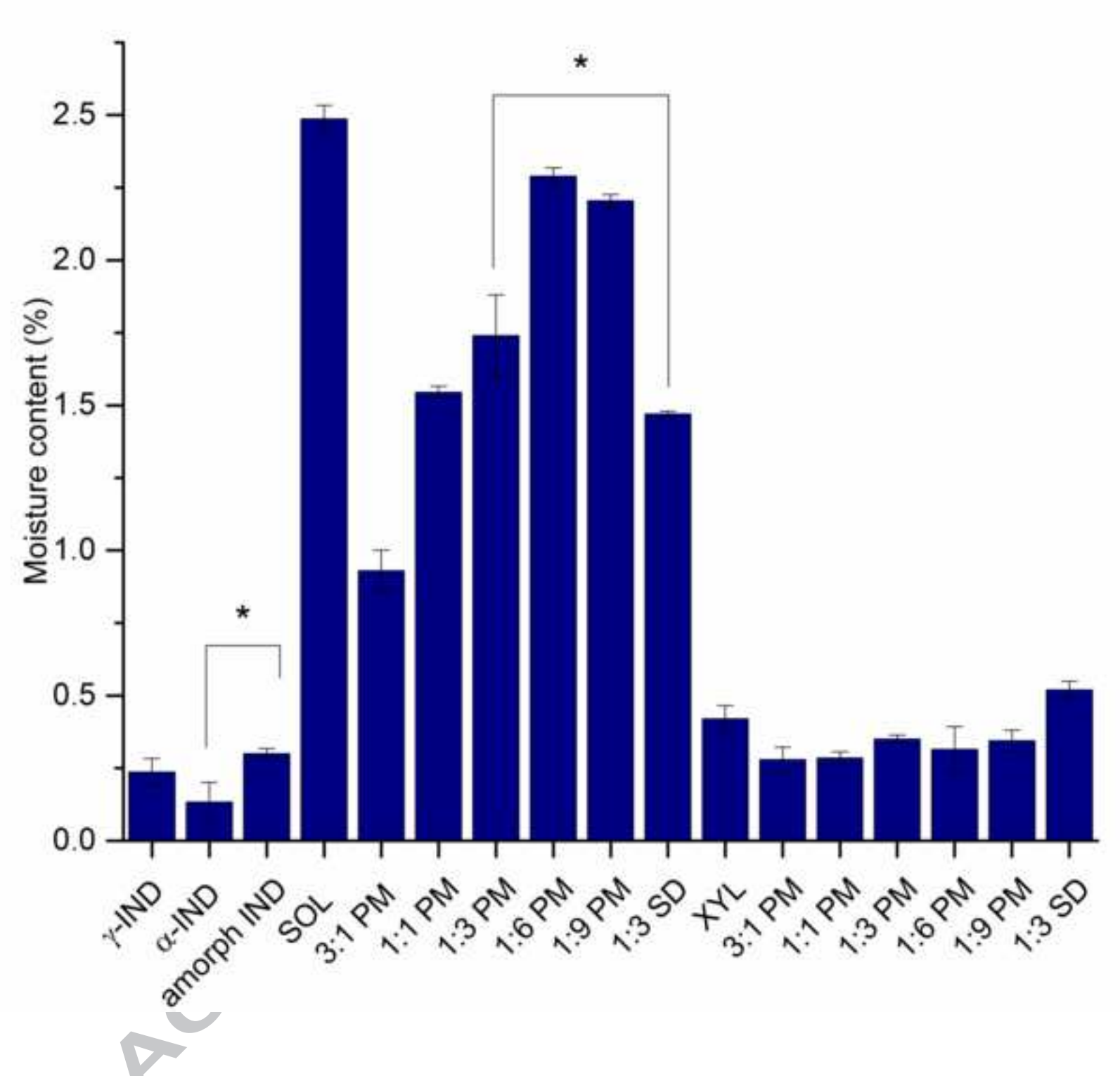

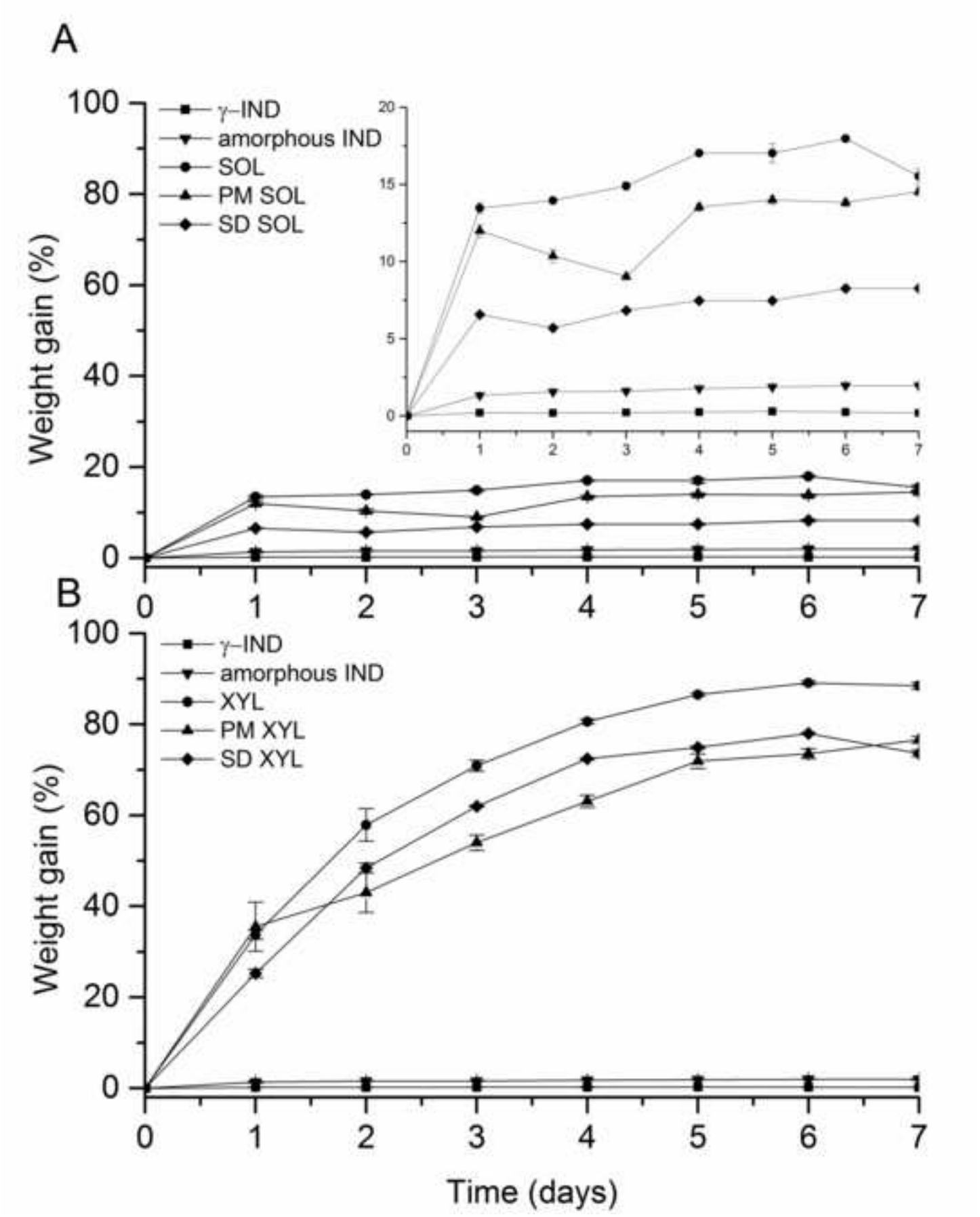
A
γ–IND
amorphous IND
SOL
PM SOL
SD SOL
Weight gain (%)
B
γ–IND
amorphous IND
XYL
PM XYL
SD XYL
Weight gain (%)
Time (days)

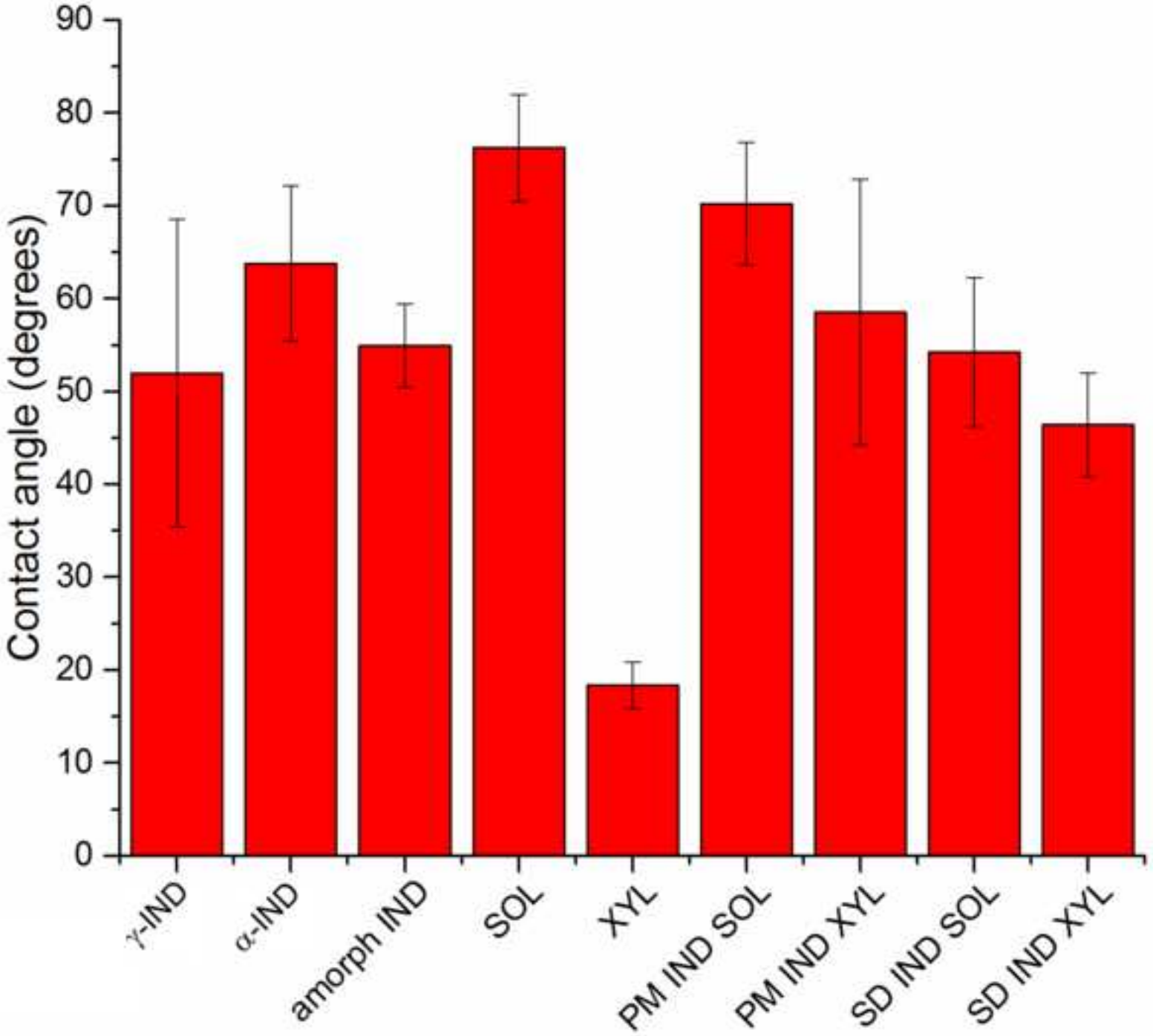

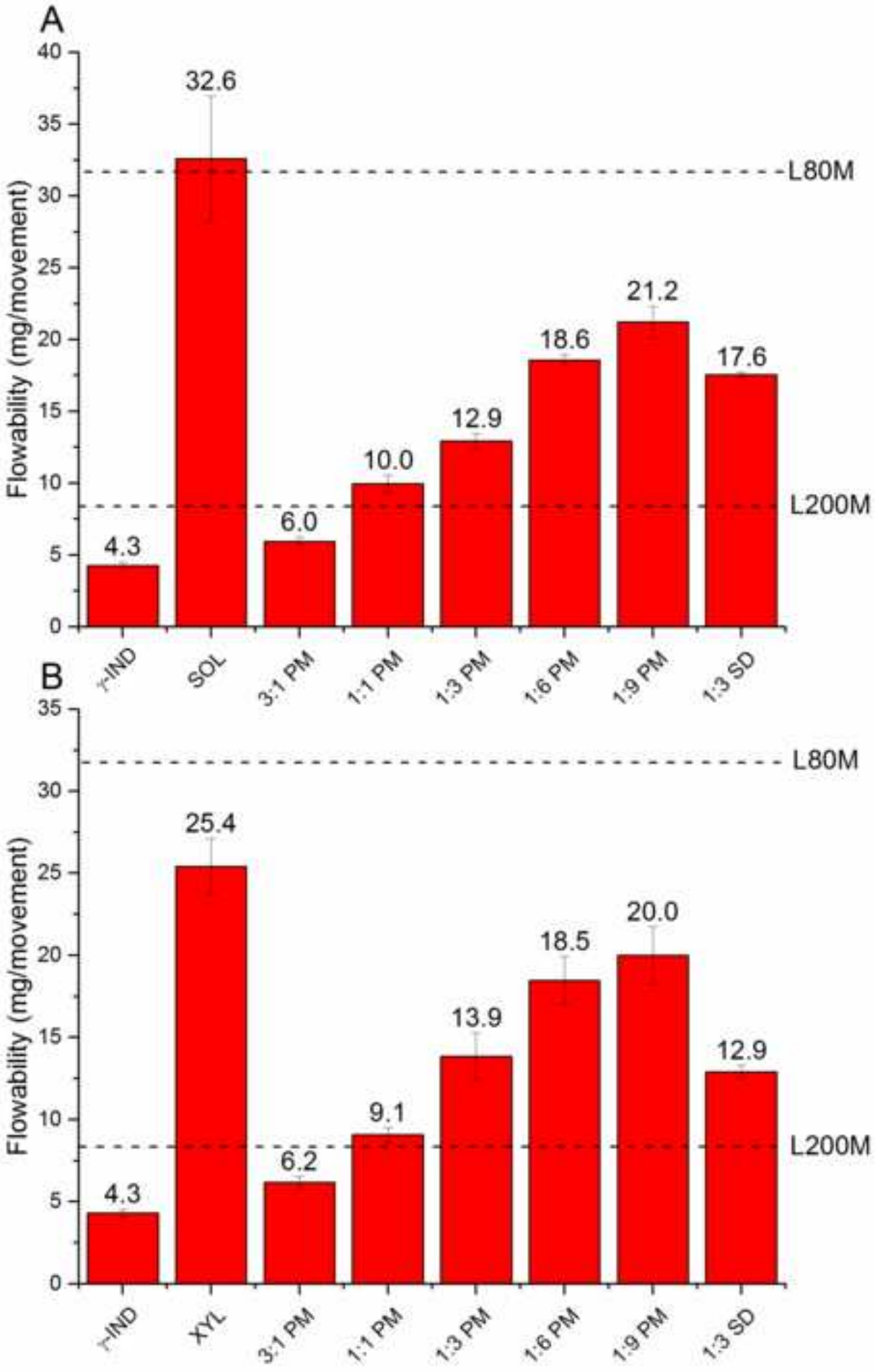
A
Flowability (mg/movement)
40
35
30
25
20
15
10
5
0
32.6
4.3
6.0
10.0
12.9
18.6
21.2
17.6
L80M
L200M
SOL
3:1 PM
1:1 PM
1:3 PM
1:6 PM
1:9 PM
1:3 SD
B
Flowability (mg/movement)
35
30
25
20
15
10
5
0
25.4
4.3
6.2
9.1
13.9
18.5
20.0
12.9
L80M
L200M
XYL
3:1 PM
1:1 PM
1:3 PM
1:6 PM
1:9 PM
1:3 SD

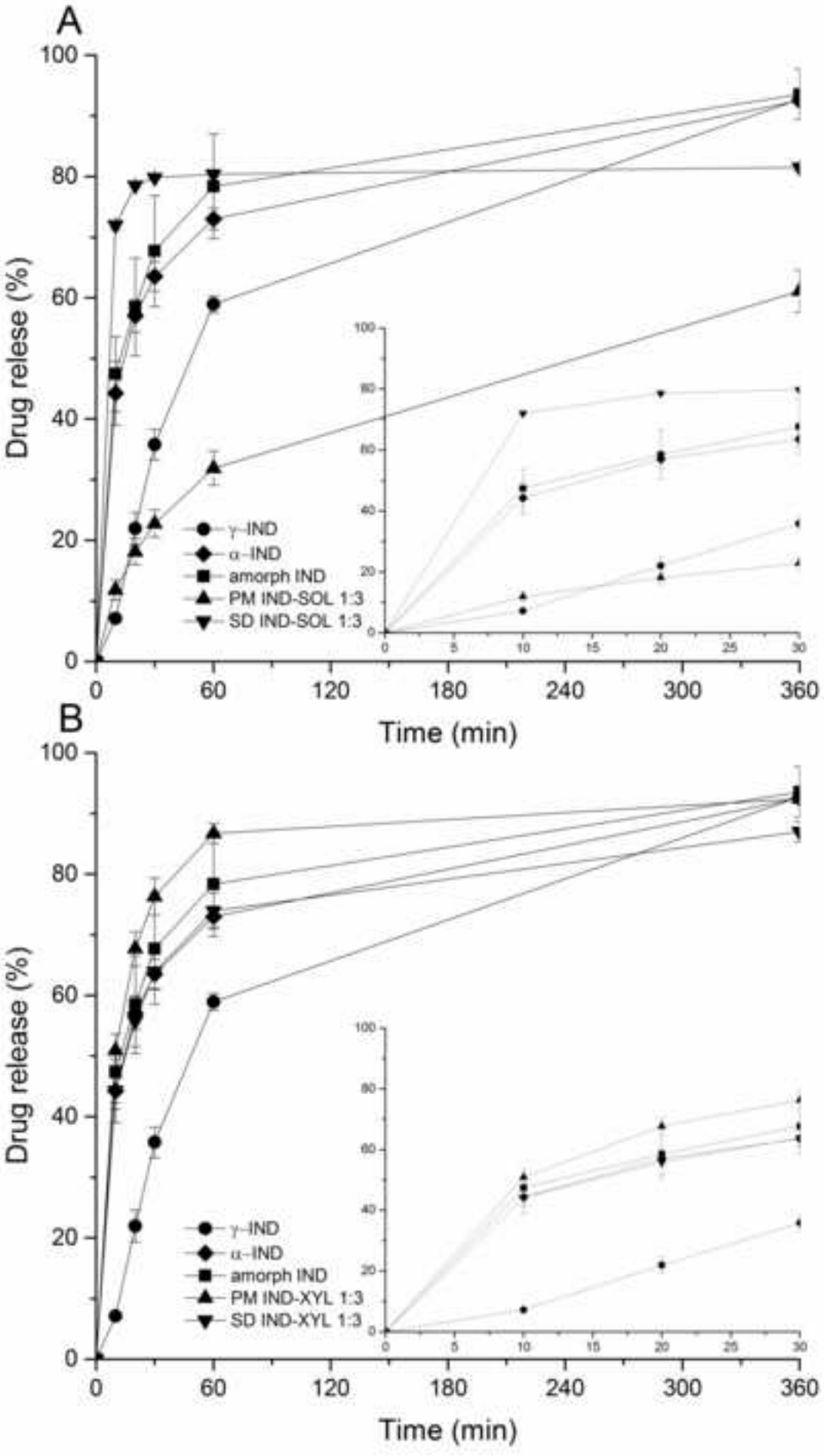
A
Drug relese (%)
Time (min)
γ-IND
α-IND
amorph IND
PM IND-SOL 1:3
SD IND-SOL 1:3
B
Drug release (%)
Time (min)
γ-IND
α-IND
amorph IND
PM IND-XYL 1:3
SD IND-XYL 1:3